


RESEARCH

Open Access



Optical coherence tomography angiography for microaneurysms in anti-vascular endothelial growth factor treated diabetic macular edema

Tongmei Zhang¹, Shiyong Xie¹, Xiaoli Sun¹, Hongtao Duan¹, Ying Li¹ and Mei Han^{1*} 

Abstract

Background We aimed to evaluate microaneurysms (MAs) after treatment with anti-vascular endothelial growth factor (anti-VEGF) therapy to understand causes of chronic edema and anti-VEGF resistance.

Methods Patients with non-proliferative diabetic retinopathy, with or without macular edema were recruited. Optical coherence tomography angiography (OCTA) MAs-related parameters were observed, including the maximum diameter of overall dimensions, material presence, and flow signal within the lumen. OCTA parameters also included central macular thickness (CMT), foveal avascular zone, superficial and deep capillary plexuses, and non-flow area measurements on the superficial retinal slab.

Results Overall, 48 eyes from 43 patients were evaluated. CMT differed significantly between the diabetic macular edema (DME) and non-DME (NDME) groups at 1st, 2nd, 3rd, and 6th months of follow-up ($P < 0.001$; < 0.001 ; 0.003 ; < 0.001 , respectively). A total of 55 and 59 MAs were observed in the DME (mean = $99.40 \pm 3.18 \mu\text{m}$) and NDME (mean maximum diameter = $74.70 \pm 2.86 \mu\text{m}$) groups at baseline, respectively (significant between-group difference: $P < 0.001$). Blood flow signal was measurable for 46 (83.6%) and 34 (59.3%) eyes in the DME and NDME groups, respectively (significant between-group difference: $P < 0.001$).

Conclusions Compared to the NDME group, the DME group had larger MAs and a higher blood-flow signal ratio. Following anti-VEGF therapy, changes in the diameter of MAs were observed before changes in CMT thickness.

Highlights

- Microaneurysms (MAs) in diabetic macular edema (DME) are not fully understood.
- We utilized optical coherence tomography angiography (OCTA) to assess the parameters of MAs.
- Changes in MAs diameter reflected the therapeutic effects of Anti-Vascular Endothelial Growth Factor (anti-VEGF) therapeutic effects.
- A limited number of MAs exhibited wall reflex shifts, as well as low content and blood flow signals.
- Anti-VEGF therapy can enhance rich blood flow signals, however, it does not improved content proportion.

Keywords Diabetic macular edema, OCT angiography, Microaneurysms (MAs), Vascular endothelial growth factor, Non-proliferative diabetic retinopathy

*Correspondence:

Mei Han

hanmay69@hotmail.com

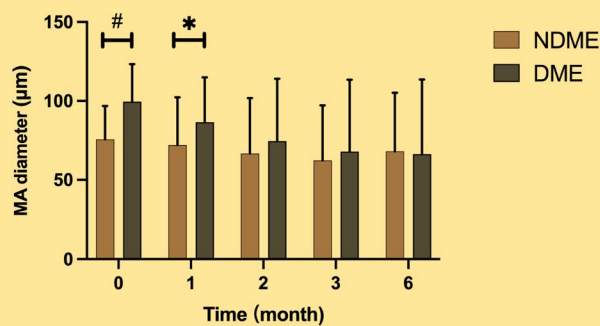
Full list of author information is available at the end of the article



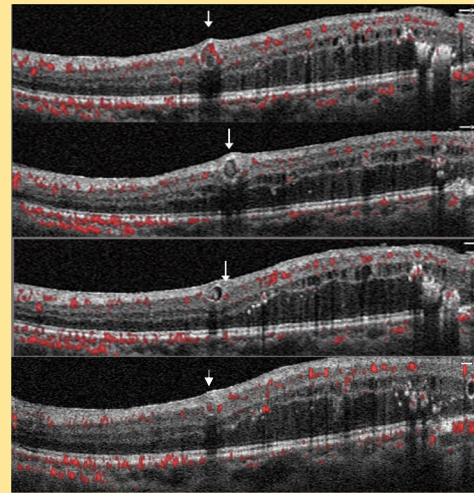
© The Author(s) 2024. **Open Access** This article is licensed under a Creative Commons Attribution-NonCommercial-NoDerivatives 4.0 International License, which permits any non-commercial use, sharing, distribution and reproduction in any medium or format, as long as you give appropriate credit to the original author(s) and the source, provide a link to the Creative Commons licence, and indicate if you modified the licensed material. You do not have permission under this licence to share adapted material derived from this article or parts of it. The images or other third party material in this article are included in the article's Creative Commons licence, unless indicated otherwise in a credit line to the material. If material is not included in the article's Creative Commons licence and your intended use is not permitted by statutory regulation or exceeds the permitted use, you will need to obtain permission directly from the copyright holder. To view a copy of this licence, visit <http://creativecommons.org/licenses/by-nc-nd/4.0/>.

Graphical Abstract

Optical coherence tomography angiography for microaneurysms in diabetic macular edema



Conclusion: Diabetic macular oedema (DME) group had larger microaneurysms (MAs) and higher blood-flow signal ratio than non-DME (NDME) group. Post anti-vascular endothelial growth factor (anti-VEGF) therapy, MAs diameter responded better than central macular thickness (CMT).



Background

Diabetes can lead to severe ocular microangiopathy, with diabetic macular edema (DME) being one of the leading causes of vision-threatening complications [1–3]. For patients with DME, anti-vascular endothelial growth factor (anti-VEGF) therapy is the primary intravitreal treatment, proving more effective in ameliorating symptoms than other therapeutic options [4]. However, many issues associated with DME remain unsolved. Additionally, some patients exhibit either poor or no response to anti-VEGF [5, 6].

Microaneurysms (MAs) are saccular outpouching originating from the retinal capillary system and are a clinically detectable sign of early diabetic retinopathy [7]. The histopathological features of MAs include saccular, fusiform, and focal bulging. The intracavitary structure is manifold, ranging from red blood cells to inflammatory cells and lipids. Basement membranes and endothelial cells also exhibit different morphologies [8].

MAs typically appear as high-fluorescence spots on fluorescein angiography (FA), but this high-fluorescence may only indicate leaky spots in retinal capillaries [9]. Furthermore, in patients with DME, late-stage leakage often becomes diffuse in the macular area, complicating the determination of MAs shape and location. Optical

coherence tomography angiography (OCTA) reveals saccular or fusiform local dilations originating from the capillaries, similar in morphology to MAs observed microscopically [8, 10]. OCTA can visualize deep blood vessels, which is impossible with FA. More importantly, OCTA's quantitative analysis of macular ischemia may be an important biomarker [11]. The technique allows for non-invasive examinations and rapid image acquisition, playing a vital role in monitoring patient recovery in DME. Additionally, the causal relationship between the formation of MAs and the stagnation of capillaries found in their vicinity remains to be investigated [12]. Hence, we also evaluated the non-perfusion range index in the detection area.

The leakage of capillaries is usually caused by the breakdown of the blood-retinal barrier, which is also responsible for the occurrence of MAs [13, 14]. The retina can also develop intracellular (and extracellular) edema as a result of ischemia [3]. Macular edema and microvascular changes can be observed by optical coherence tomography (OCT) and OCTA.

Numerous studies have attempted to elucidate the characteristics of microvessels, specifically MAs, using OCT and OCTA in patients with DME [9, 15–18]. MAs are often associated with conspicuous edema and,

therefore, a poor response to anti-VEGF [9, 15]. While the morphological and constituent characteristics of MAs are well described, the boundary of large MAs [16, 19] and the changes that occur after anti-VEGF therapy remain unclear. Some reports attempted to distinguish macroaneurysms from MAs, defining macroaneurysms as larger than 150 μm . These reports observed that laser photocoagulation was effective for larger MAs [16]. To avoid confusion, it has been proposed that macroaneurysms should be called telangiectatic capillaries (TCs) [19]. TCs are defined as large lesions with prolonged, focal indocyanine green (ICG) staining. However, clusters of small ICG-stained TCs, each < 150 μm , have also been observed [19]. This designation attempts to distinguish between MAs and macroaneurysms in ICG, but size alone is not a definitive criterion.

This study used OCT and OCTA to observe the characteristics of macular microvascular markers in patients with and without DME. The size, occurrence depth, and contents of MAs were assessed during different periods.

Subjects, materials and methods

Patients

We retrospectively reviewed the charts of patients with severe non-proliferative diabetic retinopathy (NPDR), with or without macular edema, treated at Tianjin Eye Hospital (Tianjin, China) between January 2019 and December 2021. Patients with Type 1 and Type 2 diabetes mellitus were included.

This review adhered to the principles outlined in the Declaration of Helsinki and was approved by the Ethics Committee of Tianjin Eye Hospital. Written informed consent was obtained from all patients (Table 1). The inclusion criteria were: (1) Age ≥ 18 years; (2) present of NPDR with localized or diffuse macular leakage in FA; (3)

baseline best-corrected visual acuity (BCVA) over 20/40. The exclusion criteria were: (1) prior vitrectomy surgery and/or sclera buckling surgery; (2) active proliferative diabetic retinopathy; (3) prior treatment with angiogenesis inhibitors; (4) prior intravitreal or periocular corticosteroid injections; (5) Panretinal laser photocoagulation (PRP) performed over 1 month ago; (6) poor fundus and OCTA image quality (scan quality index < 5/10); (7) prior idiopathic or autoimmune uveitis; (8) Equivalent spherical diopter $\geq -8.00\text{D}$ before refractive correction or cataract surgery; (9) Pregnancy or breastfeeding during the study; and (10) Mild or moderate NPDR.

Patients were divided into two groups based on their initial central macular thickness (CMT), which refers to the average thickness of the central 1-mm circle centered on the fovea, as measured in the Early Treatment diabetic Retinopathy Study (ETDRS) grid. Patients with CMT above 300 μm at baseline and the 6-month follow-up were assigned to the DME group. Those with CMT ≤ 300 μm at baseline and the 6-month follow-up were assigned to the NDME group [20].

Study protocol

Each patient underwent BCVA, fundus photography (FP) or, FA (HRA2, Heidelberg Eng., Germany), OCT, and OCTA at baseline. BCVA measured using the Snellen chart, was recorded as log minimal angle of resolution (MAR) visual acuity (VA). At each follow-up visit (1st, 2nd, 3rd, and 6th months), BCVA, OCT, and OCTA were repeated to assess progress. The foveal microvasculature was assessed using both OCTA and FA to determine anatomical and functional changes. FA and OCT were used to determine the presence of DME.

The eyes in the DME group were followed-up at the 1st, 2nd, 3rd, and 6th months. In the first 3 months of

Table 1 Demographic and clinical characteristics of study participants in DME and NDME group

Group	DME	NDME	p-value
Variable, n (eyes)	24	24	
Gender(yes / total)			
Male	13(54.2%)	12(50.0%)	0.500
Female	11(45.8%)	12(50.0%)	
Duration DM (years, Mean \pm SD)	16.40 \pm 6.37	14.58 \pm 8.80	0.539
Age (years, Mean \pm SD)	52.79 \pm 13.03	55.08 \pm 10.11	0.499
Diabetes type (yes / total)			
Type 1	2(8.3%)	0(0%)	0.489
Type 2	22(91.7%)	24(100%)	
Diabetic retinopathy stage (yes / total)	24(100%)	24(100%)	
Prior treatment, yes / total)			
Panretinal photocoagulation	24(100.0%)	24(100.0%)	1.000
Micropulse photocoagulation(yes / total)	1(4.1%)	1(4.1%)	1.000

follow-up, a 2 mg/0.05 mL anti-VEGF injection (Aflibercept, Eylea, Vetter Pharma-Fertigung GmbH & Co.KG, Germany) was administered monthly. Subsequently, treatment followed an as-needed protocol (PRN). Anti-VEGF treatment was administered once every 4 weeks to reduce central retinal thickness (CRT) — the average thickness over the 1-mm diameter central subfield within the ETDRS circle that is often used in studies involving OCT— to $< 300 \mu\text{m}$. If CRT remained over $300 \mu\text{m}$, injections were continued. Anti-VEGF therapy was resumed when the disease reappeared and became active. Monthly follow-up was adopted when the disease was not active [21–23].

The NDME group was enrolled within 6 months of the initial clinic visit, and their condition remained stable without macular edema. Follow-up visits were scheduled at the 1st, 2nd, 3rd, and 6th months after the initial visit.

PRP is considered an effective treatment for reducing severe visual impairment in patients with severe NPDR [24, 25]. All patients received PRP before enrolment. Micro-pulse photocoagulation was usually used in patients with central foveal thickness (CFT) —the thickness at the exact fixation point of the retina as measured on OCT scans—of less than $400 \mu\text{m}$ [26]. In this study, one person in each of the DME (CMT $347 \mu\text{m}$) and NDME (CMT $302 \mu\text{m}$) groups received micro-pulse laser treatment.

OCTA parameters

OCTA images were obtained using an AngioVue (Optovue RTVue XR Avanti System; Optovue Inc., Fremont, CA 94538, USA) machine. HD $6 \times 6 \text{ mm}^2$ scans centered on the fovea were used, with each B-scan comprising 400 A-scans. The CMT on OCTA was defined as the average full retinal thickness (from the internal limiting membrane [ILM] to the retinal pigment epithelium [RPE]) over the 1 mm diameter central subfield in the ETDRS

circle. In FA analysis of the retina, the center of the macula is generally capillary-free. This area is termed the foveal avascular zone (FAZ). The FAZ was analyzed using the Angio Retina scan 6 mm, generated based on the Retina slab (ILM to below $10 \mu\text{m}$ of the outer plexiform layer [OPL]). FAZ size, FAZ perimeter, Vessel density (VD) at the superficial capillary plexus (SCP) and deep capillary plexus (DCP), as well as the acircularity index (AI), which represents the ratio between the measured perimeter and the perimeter of the same size circular area, were all automatically calculated using the machine software. The non-flow area (NFA) was quantified semi-automatically to determine non-perfused areas on the superficial retinal slab.

MAs parameters

MAs were identified by combining OCT B-scan images with and without Angio overlay mode. Horizontal and vertical sliders were utilized to examine lines on OCT B-scan images without Angio overlay, aiming to identify cystic or circular MAs [9]. The identical spots corresponding to PFs were classified as MAs, visualized as tiny red dots. Subsequently, the diameter, blood flow signal, and contents of MAs were examined on OCT B-scan images with Angio overlay.

The maximum diameter of MAs was defined as the larger of the diameters measured in the long axial images [27] (Fig. 1). When recording the maximum diameter of the overall edge, the thickness of the MAs wall was also recorded. Multiple MAs in the same eye were numbered according to their vascular location. MAs at the corresponding location were measured during follow-up. If the MAs of the corresponding position at baseline could not be found, the diameters were recorded as zero. MAs present during follow-up but not at baseline were not recorded. To ensure consistent measurement, the auto mode of image display

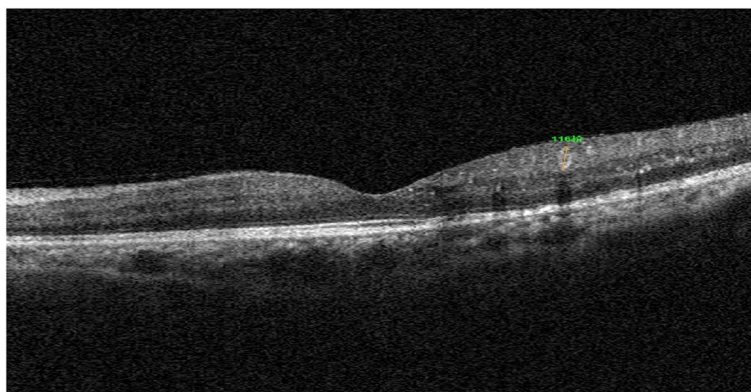


Fig. 1 The maximum diameter of MAs was defined as the larger of the diameters measured in the long axial images

was removed. The presence of material and flow signal within the lumen were simultaneously assessed using OCT. Blood flow signals in MAs were recorded as positive regardless of strength as long as they were present, as was content recording. Diameter, blood flow, and contents were primarily recorded on B-scan blood flow and B-scan OCT images although enface blood flow and enface OCT images were also crucial for MAs identification and follow-up.

Statistical analyses

All statistical analyses were conducted using SPSS Statistics Version 22.0 (IBM Statistics, v.22.0; IBM Corp, Armonk, NY). The Shapiro-Wilk test was used to check data distribution. Association between the demographic and clinical characteristics in the two experimental groups were assessed using parametric (Independent samples t-test) and nonparametric (Mann-Whitney U test and Chi-square test) tests. OCTA and MAs parameter data were compared using Generalized Estimating Equations (GEE) between the groups. For paired comparisons between each visit, the operational flow of the decomposition step in the GEE Emmeans program was modified. *P*-values < 0.05 were considered statistically significant.

Results

A total of 48 eyes from 43 patients were evaluated with 24 eyes assigned to the DME and NDME groups as described above. All 24 eyes in the DME group were treated with intravitreal ranibizumab (IVR) injections thrice monthly. The total number of injections was 3.09 ± 0.34 and 0 in the DME and NDME groups, respectively ($P < 0.001$).

Baseline BCVA was log MAR 0.69 ± 0.09 in the DME group and log MAR 0.34 ± 0.04 in the NDME group ($P < 0.001$). Significant differences in BCVA were observed between the DME and NDME groups at the 1st, 2nd, 3rd, and 6th months ($P < 0.001$; 0.001; 0.001; 0.007, respectively). CMT differed significantly between the DME and NDME groups (436.17 ± 29.95 vs. 273.33 ± 9.12 μm ; $P < 0.001$), and at each follow up month ($P < 0.001$; < 0.001; 0.003; < 0.001). No significant between-group differences existed in the OCTA-derived parameters (FAZ area, SCP VD, DCP VD, NFA) (Table 2).

In the DME group, DCP VD was lower at the 2nd month than that at the 1st month (40.80 ± 0.71 vs. 42.33 ± 0.81 ; $P = 0.043$). The NDME group had the lowest DCP VD in the 2nd month (42.33 ± 0.81) and the highest DCP VD in the 3rd month (44.06 ± 1.19). The NDME group had the lowest NFA in month 2 (1.83 ± 0.29 mm^2).

A total of 55 MAs (24 eyes) were observed in the DME group (mean maximum diameter = 99.40 ± 3.18

Table 2 OCT angiography parameters at baseline and after injections of aflibercept in the DME and NDME group

Time (month)		0	1	2	3	6
BCVA (log MAR)	DME	0.69 ± 0.09	0.70 ± 0.08	0.64 ± 0.08	0.70 ± 0.08	0.64 ± 0.08
	NDME	0.34 ± 0.04	0.33 ± 0.04	0.33 ± 0.04	0.39 ± 0.05	0.38 ± 0.05
	<i>p</i> -value	< 0.001	< 0.001	0.001	0.001	0.007
CMT(μm, Mean ± SD)	DME	436.17 ± 29.95	345.54 ± 22.59	378.54 ± 25.97	362.33 ± 25.00	355.75 ± 25.80
	NDME	273.33 ± 9.12	262.87 ± 6.07	262.39 ± 6.19	273.25 ± 16.30	259.88 ± 5.90
	<i>p</i> -value	< 0.001	< 0.001	< 0.001	0.003	< 0.001
FAZ area(mm ² , Mean ± SD)	DME	0.39 ± 0.02	0.37 ± 0.02	0.35 ± 0.02	0.36 ± 0.02	0.36 ± 0.02
	NDME	0.38 ± 0.03	0.37 ± 0.02	0.36 ± 0.02	0.36 ± 0.02	0.37 ± 0.03
	<i>p</i> -value	0.722	0.482	0.710	0.858	0.683
SCP(%)	DME	43.37 ± 0.71	43.67 ± 0.87	43.23 ± 0.80	44.23 ± 0.68	44.02 ± 0.76
	NDME	43.54 ± 0.95	43.62 ± 0.88	43.76 ± 0.88	43.45 ± 0.79	43.06 ± 0.89
	<i>p</i> -value	0.886	0.971	0.656	0.454	0.415
DCP(%)	DME	40.78 ± 0.70	42.33 ± 0.81	40.80 ± 0.71	41.66 ± 0.67	42.10 ± 0.91
	NDME	42.55 ± 1.10	43.19 ± 1.11	42.57 ± 1.04	44.06 ± 1.19	42.54 ± 1.14
	<i>p</i> -value	0.173	0.529	0.159	0.079	0.767
No flow area(mm ² , Mean ± SD)	DME	1.84 ± 0.31	2.03 ± 0.27	1.74 ± 0.23	2.16 ± 0.34	1.66 ± 0.24
	NDME	2.04 ± 0.35	2.07 ± 0.32	1.83 ± 0.29	1.79 ± 0.30	2.00 ± 0.33
	<i>p</i> -value	0.673	0.915	0.793	0.417	0.420

BCVA=best-corrected visual acuity; CRT=central retinal thickness; FAZ=foveal avascular zone; logMAR=logarithm of the minimum angle of resolution; SCP= superficial capillary plexus; DCP= deep capillary plexus ; NFA=non-flow area

μm). There were 59 MAs (24 eyes) in the NDME group at baseline (mean value = 74.70 ± 2.86 μm), with a significant between-groups difference ($P < 0.001$). During the follow-up, 3 MAs present in the DME group and 5 MAs present in the NDME group were absent at baseline. The DME group also had a significantly larger maximum diameter at the 1st month than the NDME group (86.59 ± 3.82 vs. 74.89 ± 3.88 $P = 0.031$) (Fig. 2). Blood flow signal was measurable for 46 (83.6%) and 34 (59.3%) MAs in the DME and NDME groups, respectively, with significant and signals differences between groups ($P < 0.001$) (Fig. 3). At baseline, 50.9% of MAs in the DME group and 49.2% in the NDME group had contents. Post-treatment, this proportion decreased in both groups, with not significant difference (Table 3).

During the whole follow-up period, the maximum diameter of MAs significantly decreased in the DME group compared to baseline ($P < 0.001$ for all). The

maximum diameter of MAs in the NDME group also decreased during follow-up, with a significant difference at the 3rd month compared to that at baseline ($P = 0.002$). The proportion of blood flow signal decreased after treatment in the DME group, and the difference was statistically significant ($P = 0.001, 0.001, 0.012, 0.006$). The proportion of blood flow signal increased in the NDME group after follow-up. Except for the 6th month, the NDME group's content proportion decreased ($P = 0.041, 0.040, 0.003$). No significant changes in this parameter were recorded in the DME group.

The vessel wall of the MAs was fuzzy before treatment, with evident intraluminal material (83.6% flow signal numbers, 50.9% internal components numbers). Post-treatment, the MAs walls became more defined, but the blood flow signal disappeared, and a decrease in intraluminal material within the MAs was also observed. The flow signal consistency was 62.3% in the 1st month, 62.3%

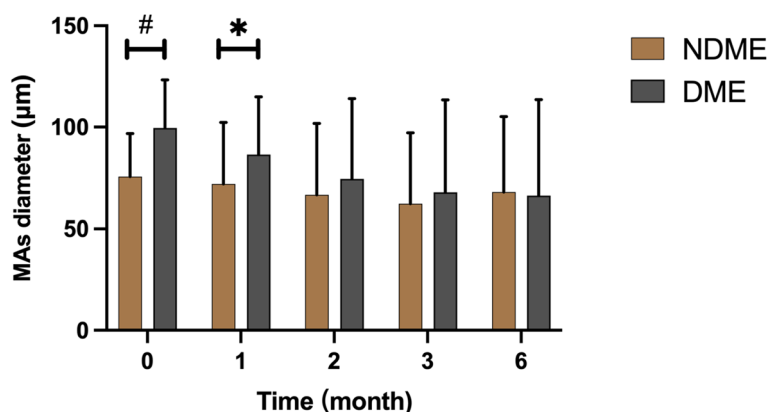


Fig. 2 The MAs maximum diameter of NDME and DME groups decreased during the follow-up period. Significant differences were observed between the two groups at pre-treatment and the 1st month ($^{\#}P < 0.01, *P < 0.05$)

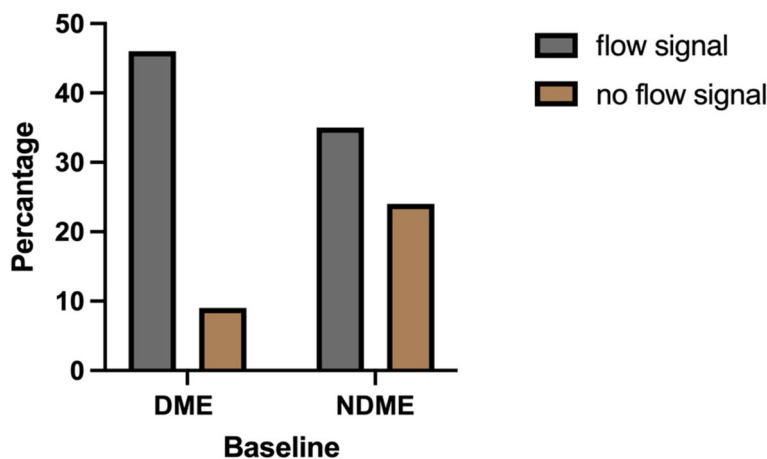


Fig. 3 Blood flow signal was measurable for 46 (83.6%) and 35 (59.3%) MAs in the DME and NDME groups, respectively, and signals differed significantly between groups ($P < 0.001$)

in the 2nd month, and 66.0% in the 3rd month. In contrast, the internal components exhibited rates of 43.4% in the 1st month, 50.9% in the 2nd month, and 39.6% in the 3rd month. Six months post-treatment, the MAs walls remained transparent, with faint blood flow signal (68.6% flow signal numbers, 39.2% internal components numbers). The maximum diameter also decreased (Figs. 4, 5, 6 and 7). The proportion of blood flow signal increased in the NDME group during the follow-up period. The maximum diameter of MAs was 161 μm in the DME group

and 133 μm in the NDME group at baseline. At follow-up, the maximum values were 181 μm and 138 μm in the DME and NDME groups, respectively.

Discussion

The effectiveness of anti-VEGF in improving visual acuity and reducing edema has previously been demonstrated [28]. Our results also revealed that both visual acuity and CMT were improved to varying degrees in the DME group.

Table 3 MAs arguments at baseline and after injections of aflibercept of OCTA in the DME and NDME group

Time (month)		0	1	2	3	6
maximum diameter , Mean ± SD)	DME	99.40±3.18	86.59±3.82	74.50±5.37	67.91±6.19	66.03±6.48
	NDME	76.84±2.86	74.89±3.88	70.98±4.40	65.24±4.41	70.12±4.71
	<i>p-value</i>	< 0.001	0.031	0.614	0.729	0.546
flow signal numbers (yes / total)	DME	46 (83.6%)	33 (62.3%)	33 (62.3%)	35 (66.0%)	35 (68.6%)
	NDME	35 (59.3%)	34 (57.6%)	35 (59.3%)	38 (64.4%)	38 (70.4%)
	<i>p-value</i>	0.001	0.283	0.610	0.461	0.885
internal components (yes / total)	DME	28/55 (50.9%)	23/53 (43.4%)	27/53 (50.9%)	21/53 (39.6%)	20/51 (39.2%)
	NDME	29/59 (49.2%)	22/59 (37.3%)	20/59 (33.9%)	18/59 (30.5%)	21/54 (38.9%)
	<i>p-value</i>	0.901	0.595	0.111	0.375	0.771

MAs= microaneurysms

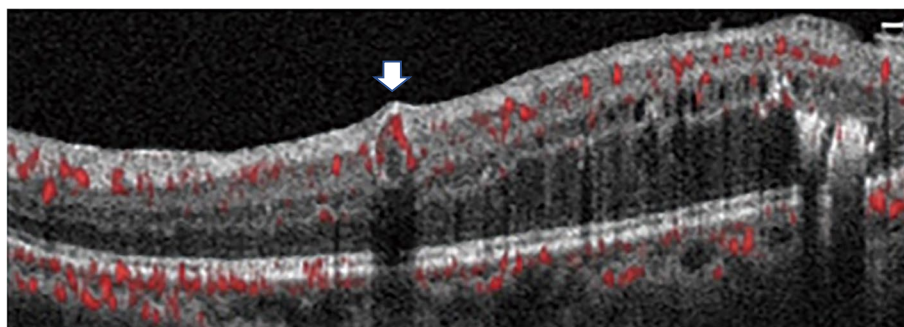


Fig. 4 The tube wall of the microaneurysms (arrow) was fuzzy before treatment, and the internal filling of the mass was evident

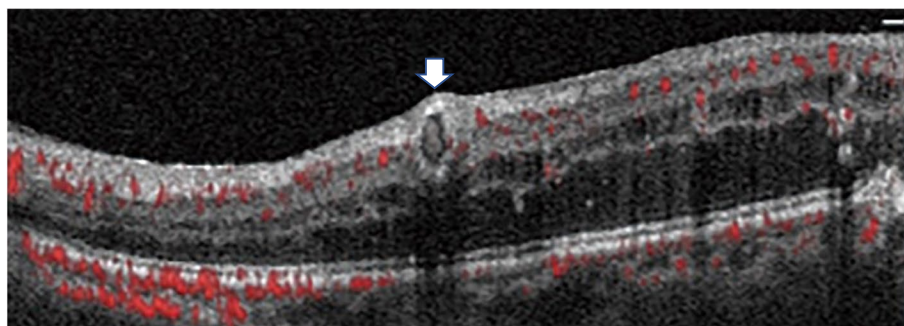


Fig. 5 The 1st month after treatment, the tube wall of the microaneurysms (arrow) became clearer during treatment, but the blood flow signal disappeared. There was also a decrease in the internal components in the tube

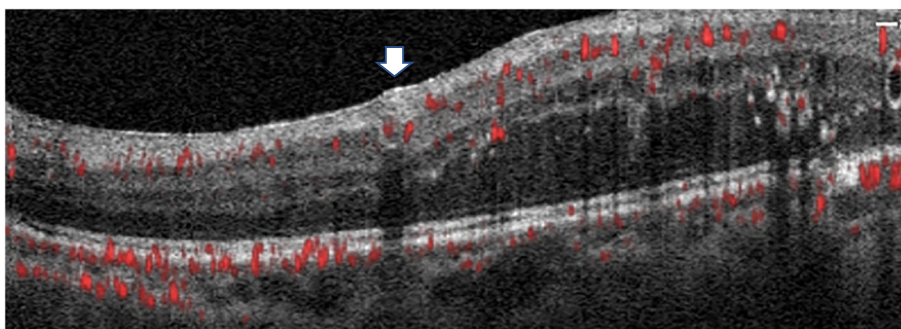


Fig. 6 The 3rd month after treatment, the tube wall of the microaneurysms (arrow) became blurry again. The blood flow signal was faint, and the components filled the tube

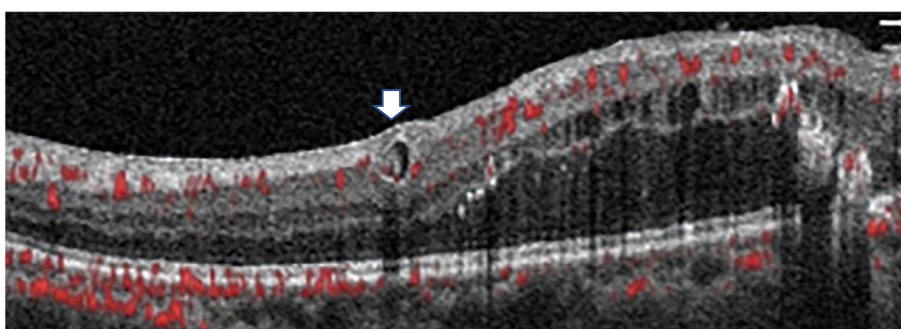


Fig. 7 The 6th month after treatment, the wall of microaneurysms (arrow) was still clear, but there was a faint signal of blood flow. The maximum diameter has also been decreased

Visual acuity was worse in the DME group than in the NDME group but improved post-treatment. No significant difference was observed in global follow-up time between the two groups. Similarly, a prior study also reported a significantly lower visual acuity in the DME group than in the NDME group (mean log MAR 0.605 ± 0.383 vs. 0.18 ± 0.247 , $P=0.001$) [29]. We also found that the FAZ area was larger in the DME than the NDME group at baseline, consistent with a previous study [30], although the difference was not significant.

A limitation of FA is extensive leakage, which not only obscures capillary dropout but also mimics MAs [31]. Therefore, applying FA might not be favorable for clinical management at all stages of the disease [32]. Additionally, some MAs were not visualized on the OCTA enface images [33]. Consequently, combining OCT B-scan with and without Angio overlay mode proves to be a helpful method for detecting MAs [31].

The maximum diameter of the MAs was reduced in the DME and NDME groups, with no difference between the groups after the 2nd month. Generally, the magnitude of the changes in MAs size varies with changes in edema height. However, the pattern of changes in MAs in the study was inconsistent with that of CMT. From

our experience, CMT is higher in DME than in NDME. Patients are screened while edema from treatment remains, up to the 6 months post-treatment, leading to increased CMT. Despite this, the maximum diameter of the treated MAs in patients with DME did not significantly differ from that in patients with NDME. The maximum diameter of MAs reached the same level in patients without edema before changes in CMT were observed, which was an indicator of good responses. Although MAs are similar to CMT, they differ in several ways.

Pre-treatment, the ratio of blood flow signal was higher in the DME than the NDME group. Post-treatment, the ratio of blood flow signal in the DME group decreased significantly post-treatment, while it remained stable in the NDME group.

However, the proportion of contents in the NDME group decreased more significantly.

The manifestation of MAs can be analyzed from anatomical appearance. Histologically, the anatomical manifestations of MAs are roughly classified as parenchyma cell type and sclerotic type [8].

According to the ultrastructural changes, MAs can be divided into four stages [8]. The following were observed in our DME group: The tube wall of the MAs was fuzzy

pre-treatment, and the internal filling of the mass was evident. This corresponded to a thin-walled type, similar to the type 1. Transmission electron micrographs of type 1 microaneurysms showed inflammatory cells in the lumen. The endothelial cells remained intact, and the basement membrane was slightly thickened. One month post-treatment, the tube wall of the MAs became clearer during treatment, but the blood flow signal disappeared, and there was also a decrease in the internal components in the tube. This was a parenchymatous type, similar to type 2 in anatomy, which was full of red blood cells. Three months post-treatment, the tube wall of the microaneurysms (arrow) became blurry again. The blood flow signal was faint, and components filled the tube, which was similar to type 3. Six months post-treatment, the tube wall remained clear, but there was only a faint blood flow signal. The maximum diameter was also decreased. This corresponded to a sclerotic type, similar to type 4, where the MAs are almost completely sclerotic, and the macrophages contain a lot of lipids (Fig. 8).

A decrease in blood flow caused by thickening of the vessel wall and accumulation of intraluminal material is considered to contribute to the poor detection of MAs [19]. The overall changes after treatment were wall thickening, increased contents, and decreased blood flow. Hence, the walls of the tubes became apparent due to the accumulation of filler, caused a decrease in blood flow. In the NDME group, MAs consistently manifested the morphology of type 2 or type 3 filled with red blood cells.

The formation of MAs is due to the loss of vascular smooth muscles and the failure of retinal vascular self-regulation, which increases the downstream capillary hydrostatic pressure. The combined effects of the absence of pericytes and increased capillary hydrostatic pressure

lead to capillary weakness and formation of formation of MAs. Patients with DR release inflammatory cytokines (upregulated ICAM and VCAM), which damage the endothelium. Without endothelial cells, red blood cell aggregation occurs. The anticoagulant factors secreted by endothelial cells can cause the formation of blood clots [8].

During follow-up visits evaluating the same site, it was challenging to find MAs with clear boundaries. Post-treatment, MAs manifest dynamically. MAs are caused by the weakening of vessel walls and can be accompanied by pericytes and endothelial cells proliferation [34]. Furthermore, MAs are traditionally considered to represent local stagnation of the retinal circulation and are a direct result of downstream hypoxia and ischemia in the retina [35]. During retinal ischemia, growth factors are released, and paracrine effects of these factors can lead to a recanalization of some MAs in those regions. The special condition of type 3, mentioned in this article, is endotheliosis, which suggests a potential possibility for vascular regeneration. Notably, when DCP VD decreased at the 2nd month post-treatment, MAs were filled with red blood cells, further explaining the relationship between ischemia and MAs.

MAs was recanalized, and the proportion of measurable blood flow was increased. Increased incidence of neonatal MAs has been associated with measurable blood flow ratios in some cases. Levin et al. [36] speculated that there could be viable and recoverable tissues in the ischemic area, which have the potential of reperfusion and could reverse retinal ischemia.

The accessory vessels that produced giant capillary aneurysms remained unobstructed after photocoagulation, suggesting that the aneurysm is saccular. This

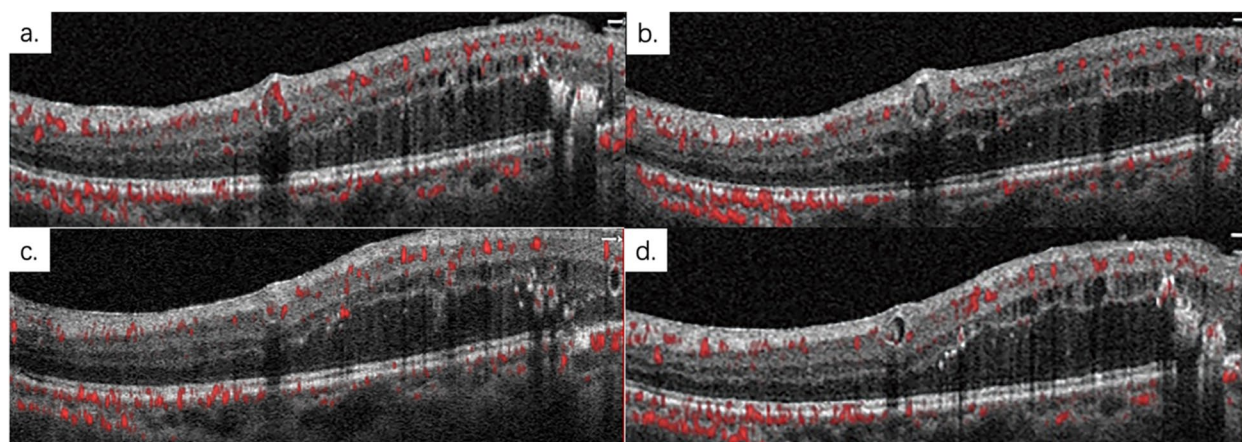


Fig. 8 **a** The baseline MAs resemble type 1 pathological features, characterized by thin walls, which are full of monocyte and poly-morphonuclear leucocytes. **b** The 1st-month MAs resembled type 2 in anatomy, which are full of red blood cells. **c** The 3rd month MAs were akin to type 3, distinguished by a fuzzy tube wall. **d** The 6th month MAs resembled type 4, indicative of a sclerotic type

implies that a large aneurysm may be a lateral dilation of the parent vessel [8]. This also explains why the contents of MAs were reduced.

MAs may not respond well to anti-VEGF therapy, therefore, laser photocoagulation is recommended for capillary MAs [18]. We also observed that the maximum diameter of MAs in the NDEM group throughout the entire visit period was 138 μm , consistent with the criteria for laser therapy. This value at least represented the upper limit of the stable state of MAs [15].

Moreover, the maximum diameter of MAs in the DME group was 181 μm , but it has been observed that MAs over 150 microns, named “macroaneurysms”, are derived from MAs because OCT and indocyanine green angiography (ICGA) phenotypes are similar. ICGA, used for identifying telangiectatic capillaries in diabetic macular edema [19], also referred to large microvascular abnormalities as telangiectatic capillaries (TCs), emphasizing the importance of ICGA in identifying MAs.

Previous research sought to distinguish larger aneurysmal changes from MAs due to differences in clinical presentation and treatment options [15, 19]. However, MAs over 150 μm , “Macroaneurysms”, are derived from MAs because OCT and ICGA phenotypes are similar [16, 19]. Since targeting lesions with photocoagulation < 130 μm yields limited vision improvement, it may be recommended to target larger lesions [16]. As earlier stated, we observed that the maximum diameter of MAs in the NDEM group during the entire visit period was 138 μm , representing the upper limit of consistent with the above criteria for laser therapy. This value at least represented the stable state of MAs. The median MAs size reported in patients with CME from DR and retinal vein occlusion (RVO) was 410 μm (range, 158–603) [16]. Whereas our DME group’s maximum MAs size was 181 μm . This discrepancy could be due to several reasons. First, we collected only structural changes in the macular region within a $6 \times 6 \text{mm}^2$ area, excluding MAs in other areas. Second, RVO patients were not included in our study, potentially affecting the value.

This study had some limitations. First, we did not focus on proliferative DR, which is difficult to assess via image analysis because severe vitreous hemorrhages often accompany it. Second, we focused only on a limited area of MAs, which should be expanded in future studies to explore the relationship between retinal ischemia status and MAs. Third, the follow-up time after anti-VEGF treatment was limited and should be in future studies.

Conclusions

Continuous analysis of refractory DME and its response to anti-VEGF treatments remains crucial. While detailed descriptions of MAs in DME via OCT and OCTA exist,

our study highlights some key observations. The DME group exhibited larger MAs and stronger blood flow signals than the NDME group. Following initiation of anti-VEGF therapy, CMT showed no difference between the two groups at month 3, while MAs diameter showed no difference at month 2. Interestingly, changes in MAs diameter preceded changes in CMT thickness, suggesting that alterations in MAs size may more directly reflect therapeutic effects. After anti-VEGF treatment, MAs diameter decreased and tended to stabilize, although complete resolution was more challenging in the DME group, potentially contributing to treatment-resistant edema. Anti-VEGF therapy also improved the richness of blood flow signals.

Post-treatment, the morphology of MAs contents dynamically changed, with some patients exhibiting clearer wall reflexes, reduced contents, and decreased blood flow signals. This process likely involves absorbing accumulated white and red blood cells, necessitating further pathological confirmation.

Abbreviations

AI	Acircularity Index
anti-VEGF	Anti-Vascular Endothelial Growth Factor
BCVA	Best-Corrected Visual Acuity
CFT	Central Foveal Thickness
CMT	Central Macular Thickness
CRT	Central Retinal Thickness
DCP	Deep Capillary Plexus
DME	Diabetic Macular Edema
ETDRS	Early Treatment Diabetic Retinopathy Study
FA	Fluorescein Angiography
FAZ	Foveal Avascular Zone
FP	Fundus Photography
GEE	Generalized Estimating Equations
ICG	Indocyanine Green
ILM	Internal Limiting Membrane
MAs	Microaneurysms
NDME	Non-Diabetic Macular Edema
NFA	Non-Flow Area
NPDR	Non-Proliferative Diabetic Retinopathy
OCT	Optical Coherence Tomography
OCTA	Optical Coherence Tomography Angiography
OPL	Outer Plexiform Layer
PRN	Pro Re Nata
PRP	Panretinal Laser Photocoagulation
RPE	Retinal Pigment Epithelium
SCP	Superficial Capillary Plexus
TCs	Telangiectatic Capillaries
VD	Vessel Density

Acknowledgements

Not applicable.

Authors’ contributions

TM.Z: Conceptualization, Methodology, Data collection, Data analysis, Writing, editing. H.M: Conceptualization, Methodology, Data collection. S.Y.X: Conceptualization. X.L.S: Data collection, Data analysis. H.T.D: Data collection, Data analysis. Y.L: Data collection, Data analysis. All authors approved the final version of the manuscript.

Funding

Supported by Tianjin Key Medical Discipline (Specialty) Construction Project (No.TJYXZDXK-016 A); Science and Technology Fund of Tianjin Eye

Hospital (No.YKZD1903); Tianjin Science and Technology Project of China (No.14JCYBJC27400).

Availability of data and materials

The datasets generated and analysed during the current study are not publicly available due to human data but are available from the corresponding author on reasonable request.

Data availability

Data is provided within the manuscript or supplementary information files.

Declarations

Ethics approval and consent to participate

The study was conducted according to the guidelines of the Declaration of Helsinki, and approved by Ethics Committee, Medicine, Tianjin Eye Hospital (Research ID: 2022016). Written informed consents were obtained from all participants.

Consent for publication

Not Applicable.

Competing interests

The authors declare no competing interests.

Author details

¹Tianjin Eye Hospital, Tianjin Key Lab of Ophthalmology and Visual Science, 4th Gansu Road, Heping District, Tianjin 30020, PR China.

Received: 30 December 2023 Accepted: 21 August 2024

Published online: 09 September 2024

References

- Teo ZL, Tham YC, Yu M, Chee ML, Rim TH, Cheung N, et al. Global prevalence of diabetic retinopathy and projection of burden through 2045: systematic review and meta-analysis. *Ophthalmology*. 2021;128(11):1580–91.
- Yau JWY, Rogers SL, Kawasaki R, Lamoureux EL, Kowalski JW, Bek T, et al. Global prevalence and major risk factors of diabetic retinopathy. *Diabetes Care*. 2012;35(3):556–64.
- Amoaku WM, Ghanchi F, Bailey C, Banerjee S, Banerjee S, Downey L, et al. Diabetic retinopathy and diabetic macular oedema pathways and management: UK Consensus Working Group. *Eye (Lond)*. 2020;34(Suppl 1):1–51.
- Schmidt-Erfurth U, Garcia-Arumi J, Bandello F, Berg K, Chakravarthy U, Gerendas BS, et al. Guidelines for the management of diabetic macular edema by the European Society of Retina Specialists (EURETINA). *Ophthalmologica*. 2017;237(4):185–222.
- Parravano M, Costanzo E, Querques G. Profile of non-responder and late responder patients treated for diabetic macular edema: systemic and ocular factors. *Acta Diabetol*. 2020;57(8):911–21.
- Usui-Ouchi A, Tamaki A, Sakanishi Y, Tamaki K, Mashimo K, Sakuma T, et al. Factors affecting a short-term response to anti-VEGF therapy in diabetic macular edema. *Life (Basel)*. 2021;11(2):83.
- Diaz JD, Oellers P, Silverman R, Miller JB. Optical coherence tomography-angiography of a large retinal microaneurysm. *Am J Ophthalmol Case Rep*. 2020;18:100690.
- Stitt AW, Gardiner TA, Archer DB. Histological and ultrastructural investigation of retinal microaneurysm development in diabetic patients. *Br J Ophthalmol*. 1995;79(4):362–7.
- Ishibazawa A, Nagaoka T, Takahashi A, Omae T, Tani T, Sogawa K, et al. Optical coherence tomography angiography in diabetic retinopathy: a prospective pilot study. *Am J Ophthalmol*. 2015;160(1):35–e441.
- Moore J, Bagley S, Ireland G, McLeod D, Boulton ME. Three dimensional analysis of microaneurysms in the human diabetic retina. *J Anat*. 1999;194(Pt 1):89–100.
- Everett LA, Paulus YM. Laser therapy in the treatment of diabetic retinopathy and diabetic macular edema. *Curr Diab Rep*. 2021;21(9):35.
- Murakami T. OCT angiography image stack casts light on multifaceted pathophysiologic features in diabetic microaneurysms. *Ophthalmol Retina*. 2020;4(2):187–8.
- Wilson CA, Berkowitz BA, Sato Y, Ando N, Handa JT, de Juan E Jr. Treatment with intravitreal steroid reduces blood-retinal barrier breakdown due to retinal photocoagulation. *Arch Ophthalmol*. 1992;110(8):1155–9.
- Klaassen I, Van Noorden CJ, Schlingemann RO. Molecular basis of the inner blood-retinal barrier and its breakdown in diabetic macular edema and other pathological conditions. *Prog Retin Eye Res*. 2013;34:19–48.
- Karti O, Ipek SC, Saatci AO. Multimodal imaging characteristics of a large retinal capillary macroaneurysm in an eye with severe diabetic macular edema: a case presentation and literature review. *Med Hypothesis Discov Innov Ophthalmol*. 2020;9(1):33–7.
- Paques M, Philippakis E, Bonnet C, Falah S, Ayello-Scheer S, Zwillinger S, et al. Indocyanine-green-guided targeted laser photocoagulation of capillary macroaneurysms in macular oedema: a pilot study. *Br J Ophthalmol*. 2017;101(2):170–4.
- Sun Z, Yang D, Tang Z, Ng DS, Cheung CY. Optical coherence tomography angiography in diabetic retinopathy: an updated review. *Eye (Lond)*. 2021;35(1):149–61.
- Nakao S, Yoshida S, Kaizu Y, Yamaguchi M, Wada I, Ishibashi T, et al. Microaneurysm detection in diabetic retinopathy using OCT angiography may depend on intramicroaneurysmal turbulence. *Ophthalmol Retina*. 2018;2(11):1171–3.
- Castro Farias D, Matsui Serrano R, Bianchi Gancharov J, de Dios Cuadras U, Sahel J, Graue Wiechers F, et al. Indocyanine green angiography for identifying telangiectatic capillaries in diabetic macular oedema. *Br J Ophthalmol*. 2020;104(4):509–13.
- Huang WH, Lai CC, Chuang LH, Huang JC, Wu CH, Lin YT, et al. Foveal microvascular integrity association with anti-VEGF treatment response for diabetic macular edema. *Invest Ophthalmol Vis Sci*. 2021;62(9):41.
- Elman MJ, Aiello LP, Beck RW, Bressler NM, Bressler SB, Edwards AR, et al. Randomized trial evaluating ranibizumab plus prompt or deferred laser or triamcinolone plus prompt laser for diabetic macular edema. *Ophthalmology*. 2010;117(6):1064–77.e35.
- Ishibashi T, Li X, Koh A, Lai TY, Lee FL, Lee WK, et al. The REVEAL study: ranibizumab monotherapy or combined with laser versus laser monotherapy in Asian patients with diabetic macular edema. *Ophthalmology*. 2015;122(7):1402–15.
- Brown DM, Schmidt-Erfurth U, Do DV, Holz FG, Boyer DS, Midena E, et al. Intravitreal aflibercept for diabetic macular edema: 100-week results from the VISTA and VIVID studies. *Ophthalmology*. 2015;122(10):2044–52.
- Singh RP, Elman MJ, Singh SK, Fung AE, Stoulov I. Advances in the treatment of diabetic retinopathy. *J Diabetes Complications*. 2019;33(12): 107417.
- Photocoagulation treatment of proliferative diabetic retinopathy. Clinical application of Diabetic Retinopathy Study (DRS) findings, DRS report number 8. The diabetic retinopathy study research group. *Ophthalmology*. 1981;88(7):583–600.
- Mansouri A, Sampat KM, Malik KJ, Steiner JN, Glaser BM. Efficacy of sub-threshold micropulse laser in the treatment of diabetic macular edema is influenced by pre-treatment central foveal thickness. *Eye (Lond)*. 2014;28(12):1418–24.
- Sugawara H, Watanabe H, Kunimatsu A, Abe O, Yatabe Y, Watanabe SI, et al. Tumor size in patients with severe pulmonary emphysema might be underestimated on preoperative CT. *Eur Radiol*. 2022;32(1):163–73.
- Maggio E, Sartore M, Attanasio M, Maraone G, Guerriero M, Polito A, et al. Anti-vascular endothelial growth factor treatment for diabetic macular edema in a real-world clinical setting. *Am J Ophthalmol*. 2018;195:209–22.
- Braham IZ, Kaouel H, Boukari M, Ammous I, Errais K, Boussen IM, et al. Optical coherence tomography angiography analysis of microvascular abnormalities and vessel density in treatment-naïve eyes with diabetic macular edema. *BMC Ophthalmol*. 2022;22(1):418.
- Di G, Weihong Y, Xiao Z, Zhikun Y, Xuan Z, Yi Q, et al. A morphological study of the foveal avascular zone in patients with diabetes mellitus using optical coherence tomography angiography. *Graefes Arch Clin Exp Ophthalmol*. 2016;254(5):873–9.
- Stattin M, Haas AM, Ahmed D, Stolba U, Graf A, Krepler K, et al. Detection rate of diabetic macular microaneurysms comparing dye-based angiography and optical coherence tomography angiography. *Sci Rep*. 2020;10(1):16274.

32. Parrulli S, Corvi F, Cozzi M, Monteduro D, Zicarelli F, Staurengi G. Microaneurysms visualisation using five different optical coherence tomography angiography devices compared to fluorescein angiography. *Br J Ophthalmol.* 2021;105(4):526–30.
33. Hamada M, Ohkoshi K, Inagaki K, Ebihara N, Murakami A. Visualization of microaneurysms using optical coherence tomography angiography: comparison of OCTA en face, OCT B-scan, OCT en face, FA, and IA images. *Jpn J Ophthalmol.* 2018;62(2):168–75.
34. Bourhis A, Girmens JF, Boni S, Pecha F, Favard C, Sahel JA, et al. Imaging of macroaneurysms occurring during retinal vein occlusion and diabetic retinopathy by indocyanine green angiography and high resolution optical coherence tomography. *Graefes Arch Clin Exp Ophthalmol.* 2010;248(2):161–6.
35. De Venecia G, Davis M, Engerman R. Clinicopathologic correlations in diabetic retinopathy. I. Histology and fluorescein angiography of microaneurysms. *Arch Ophthalmol.* 1976;94(10):1766–73.
36. Levin AM, Rusu I, Orlin A, Gupta MP, Coombs P, D'Amico DJ, et al. Retinal reperfusion in diabetic retinopathy following treatment with anti-VEGF intravitreal injections. *Clin Ophthalmol.* 2017;11:193–200.

Publisher's note

Springer Nature remains neutral with regard to jurisdictional claims in published maps and institutional affiliations.